

Article

Accumulation of Linoleic Acid by Altered Peroxisome Proliferator-Activated Receptor- α Signaling Is Associated with Age-Dependent Hepatocarcinogenesis in *Ppara* Transgenic Mice

Xiaoyang Zhu ^{1,*}, Qing Liu ¹, Andrew D. Patterson ¹, Arun K. Sharma ², Shantu G. Amin ², Samuel M. Cohen ³, Frank J. Gonzalez ⁴ and Jeffrey M. Peters ¹

¹ Department of Veterinary and Biomedical Science, The Center for Molecular Toxicology and Carcinogenesis, The Pennsylvania State University, University Park, State College, PA 16802, USA; lqing124@gmail.com (Q.L.); adp117@psu.edu (A.D.P.); jmp21@psu.edu (J.M.P.)

² Department of Pharmacology, The Pennsylvania State University, Hershey, PA 17033, USA; aks14@psu.edu (A.K.S.); sga3@psu.edu (S.G.A.)

³ Department of Pathology and Microbiology, University of Nebraska Medical Center, Omaha, NE 68198, USA; scohen@unmc.edu

⁴ Laboratory of Metabolism, National Cancer Institute, Bethesda, MD 20892, USA; gonzalef@mail.nih.gov

* Correspondence: xzz145@psu.edu; Fax: 814-863-1696

Abstract: Long-term ligand activation of PPAR α in mice causes hepatocarcinogenesis through a mechanism that requires functional PPAR α . However, hepatocarcinogenesis is diminished in both *Ppara*-null and *PPARA*-humanized mice, yet both lines develop age-related liver cancer independently of treatment with a PPAR α agonist. Since PPAR α is a master regulator of liver lipid metabolism in the liver, lipidomic analyses were carried out in wild-type, *Ppara*-null, and *PPARA*-humanized mice treated with and without the potent agonist GW7647. The levels of hepatic linoleic acid in *Ppara*-null and *PPARA*-humanized mice were markedly higher compared to wild-type controls, along with overall fatty liver. The number of liver CD4⁺ T cells was also lower in *Ppara*-null and *PPARA*-humanized mice and was negatively correlated with the elevated linoleic acid. Moreover, more senescent hepatocytes and lower serum TNF α and IFN γ levels were observed in *Ppara*-null and *PPARA*-humanized mice with age. These studies suggest a new role for PPAR α in age-associated hepatocarcinogenesis due to altered lipid metabolism in *Ppara*-null and *PPARA*-humanized mice and the accumulation of linoleic acid as part of an overall fatty liver that is associated with loss of CD4⁺ T cells in the liver in both transgenic models. Since fatty liver is a known causal risk factor for liver cancer, *Ppara*-null and *PPARA*-humanized mice are valuable models for examining the mechanisms of PPAR α and age-dependent hepatocarcinogenesis.

Keywords: peroxisome proliferator-activated receptor- α (PPAR α); hepatocarcinogenesis; linoleic acid; CD4⁺ T cell; senescence



Citation: Zhu, X.; Liu, Q.; Patterson, A.D.; Sharma, A.K.; Amin, S.G.; Cohen, S.M.; Gonzalez, F.J.; Peters, J.M. Accumulation of Linoleic Acid by Altered Peroxisome Proliferator-Activated Receptor- α Signaling Is Associated with Age-Dependent Hepatocarcinogenesis in *Ppara* Transgenic Mice. *Metabolites* **2023**, *13*, 936. <https://doi.org/10.3390/metabo13080936>

Academic Editor: Nimer Assy

Received: 10 July 2023

Revised: 3 August 2023

Accepted: 6 August 2023

Published: 10 August 2023



Copyright: © 2023 by the authors. Licensee MDPI, Basel, Switzerland. This article is an open access article distributed under the terms and conditions of the Creative Commons Attribution (CC BY) license (<https://creativecommons.org/licenses/by/4.0/>).

1. Introduction

The peroxisome proliferator-activated receptors (PPARs) are members of the steroid/nuclear receptor family. PPARs have essential roles in cellular homeostasis, differentiation, inflammation, and modulation of carcinogenesis [1,2]. PPAR α , one of three PPAR subtypes (PPAR α , PPAR β/δ , and PPAR γ) identified in 1990 [3,4] has important roles in the transport and oxidation of fatty acids in many tissues including the liver, heart, intestine, and kidney where lipids can be used as an energy source [5,6]. PPARs are ligand-activated transcription factors that dynamically regulate gene expression in response to endogenous or exogenous ligands. Ligands bind to PPAR, causing structural changes in the protein structure releasing co-factors that maintain a tight complex on chromatin and recruit other proteins to the PPAR complex to facilitate the transcription of target genes. Importantly, nuclear receptors such as PPARs exist in dynamic equilibrium between chromatin binding and an intracellular PPAR complex, due to the

presence/absence of ligands, accessory proteins, and PPARs [7,8]. It is important to note that PPAR α is the molecular target that mediates the lipid lowering effects of the widely prescribed fibrate class of hypolipidemic drugs [9]. The mechanism by which PPAR α causes a decrease in serum triglycerides by fibrates is primarily through increased expression of PPAR α target genes that facilitate the transport of fatty acids across membranes and catabolism in tissues that generates cellular ATP via oxidation of long-chain fatty acids and effectively decreases the triglycerides in serum [9–11]. Since most organisms typically exist in a fasting state where fatty acids are higher and able to bind with PPAR α , this nuclear receptor is essential for regulating lipid homeostasis [12].

While it is clear that PPAR α activation is essential for cellular energy homeostasis [9–11], pharmacological activation of the PPAR α with synthetic ligands causes hepatocarcinogenesis in rodents through a mechanism that requires PPAR α . Whereas wild-type mice which were fed a diet with the synthetic PPAR α ligands Wy-14,643, bezafibrate, or GW7647 all exhibited close to 100% incidence of liver cancer after approximately one year of treatment, *Ppara*-null mice are largely refractory to this effect [13–17]. The mechanisms that mediate this are caused by PPAR α -dependent down-regulation of let7c microRNA and E-cadherin/cadherin 1 (CDH1) in the liver that leads to higher expression of proteins that promote hepatocyte proliferation of cells with DNA damage [18–20]. Hepatocarcinogenesis is also diminished in *PPARA*-humanized mice after chronic treatment with either Wy-14,643 or GW7647 [13,14,16]. Results from studies examining the mechanism of PPAR α -dependent liver cancer also show that activation of this receptor effectively decreases serum lipids in both rodents and humans, but the changes in the let7c pathway occur only in wild-type mice, which is not found in *PPARA*-humanized mice after chronic treatment with either Wy-14,643 or GW7647 [13,14,16]. In addition to these studies, there is other strong evidence indicating that a species difference exists between rodents and humans with regard to their susceptibility to liver cancer from PPAR α ligands as rodents develop liver cancer but there is no epidemiological evidence that this occurs in humans [5,9,21,22]. Furthermore, increased hepatocellular proliferation, a key event in the mode of action of PPAR α -induced hepatocarcinogenesis in rodents, does not occur in humans, as demonstrated in the chimeric humanized mouse liver model [23].

Studies using *Ppara*-null and *PPARA*-humanized mice demonstrated an essential role for PPAR α in rodent liver cancer caused by PPAR α ligands. However, some studies have revealed that spontaneous liver tumors develop in aged *Ppara*-null and *PPARA*-humanized mice in the absence of exogenous PPAR α ligand administration [13–15,24]. Given the critical role of PPAR α in regulating lipid catabolism, it is not surprising that *Ppara*-null mice exhibit reduced constitutive expression of hepatic lipid metabolizing enzymes [25]. Liver steatosis is found in aging *Ppara*-null mice [13,14], and hepatic steatosis is well-known to be a form of hepatocellular toxicity, leading to liver inflammation and increased incidences of hepatocellular tumors in rodents and in humans [26–28]. For these reasons, the present studies were designed to test the hypothesis that alterations in hepatic lipid metabolism cause liver cancer independent of PPAR α .

2. Materials and Methods

2.1. GW7647 Synthesis

2-Methyl-2-[[4-[2-[[cyclohexylamino]carbonyl](4-cyclohexylbutyl)amino]ethyl]phenyl]thio]-propanoic acid (GW7647) was synthesized by the Penn State Cancer Institute Organic Synthesis Shared Resource as described previously [13,14,29]. The GW7647 synthesized was between 96.6 and 98.4% pure based on HPLC analyses.

2.2. Diets

Pelleted mouse chow was prepared (Dyets Inc., Bethlehem, PA, USA) containing either 0.0 (control) or 0.01% GW7647 and it was provided to mice *ad libitum*. The concentration of GW7647 was based on results showing that relative to controls, 0.01% GW7647 caused a similar increase in liver weight and hepatic expression of the PPAR α target gene *cytochrome*

P450 4a10 (*Cyp4a10*) compared to 0.1% WY-14,643 after seven days of treatment [13,14]. Tap water was available *ad libitum*.

2.3. Study Designs

The tissue samples used for these studies were obtained from two previously published studies approved by the Pennsylvania State University Institutional Animal Care and Use Committee (IACUC31363, 17 May 2011) [13,14]. Briefly, both studies used wild-type, *Ppara*-null, or *PPARA*-humanized mice on the 129/Sv genetic background as previously described [30,31]. Two exposure paradigms were used (Figure S1). The first paradigm used six- to twelve-week-old male mice, either wild-type, *Ppara*-null or *PPARA*-humanized [13,14]. Ligand activation of PPAR α was achieved by feeding the either control or 0.01% GW7647 diet to the three different lines of mice for either 26 weeks or ~75 weeks (Figure S1a). This group is referred to as “adult only”. For the second study, ligand activation of PPAR α was initiated in perinatal mice on postnatal day 3 and continued into adulthood (Figure S1b). Neonatal mice were gavaged daily with a dose of 10 mg GW7647/body weight (kilogram) from postnatal day 3 to postnatal day 21, when the mice were weaned. After postnatal day 21, the mice were fed either the control diet or one containing 0.01% GW7647 *ad libitum* like the adult mice for either 26 weeks or ~75 weeks (Figure S1b). This group is referred to as “perinatal + adult”. Exposure to chemicals during prenatal and perinatal development can alter the developing conceptus differentially compared to adults, and may cause effects that persist/manifest later in life including cancer [32]. Ligand activation of PPAR α in fetuses by clofibrate in pregnant rats causes peroxisome proliferation but younger fetuses appeared less responsive to this effect compared to fetuses exposed to clofibrate during later gestation and other studies have also noted that developing fetuses or neonates can exhibit varying levels of peroxisome proliferation and/or induction of hepatic PPAR α target genes during perinatal development [33–36]. For these reasons, the present studies examined the effect of long-term administration of a PPAR α agonist GW7647, on hepatocarcinogenesis using wild-type, *Ppara*-null, and *PPARA*-humanized mice with exposure beginning either in adult mice or those at the age of postnatal day 3. Importantly, these treatment paradigms were used to allow direct comparison between the changes in the liver metabolome in the present studies and the relative incidence of liver cancer induced in the presence or absence of a functional mouse or human PPAR α noted in previous studies [13,14].

2.4. Hepatic Metabolomics Using ^1H Nuclear Magnetic Resonance (NMR) and Data Analyses

Approximately fifty milligrams of liver tissue from mice were homogenized with a BeadBlaster Homogenizer (Southern Labware, Cumming, GA, USA) for 90 s (with a 5 s interval per 30 s) in microcentrifuge tubes containing zirconia/silica beads and pre-cooled chloroform and methanol (2:1) mixture. After one 90 s cycle, the liver tissue samples were cooled on ice for 15 min, and this procedure was repeated one more time. Samples were then centrifuged at $12,000 \times g$, 4 °C for 10 min and the supernatants containing the lipid extracts were transferred to new tubes. The lipid extracts were dried with a speed vacuum and resuspended in deuterated chloroform (CDCl_3 , 0.03% (*v/v*) tetramethylsilane (TMS); Sigma-Aldrich, St Louis, MO, USA) and then transferred into NMR tubes.

^1H NMR spectra of liver lipid extracts were acquired at 298 K using a Bruker AVIII 600 MHz NMR spectrometer (Bruker Biospin, Rheinstetten, BW, Germany) with a cryogenic probe, operating at a proton frequency of 600.13 MHz. The standard Bruker zg pulse sequence was employed for one-dimensional NMR spectra. Two-dimensional NMR spectra (^1H - ^1H COSY and TOCSY, ^1H - ^{13}C HSQC, and HMBC) were acquired to assist with the spectral assignment in addition to comparing these data with published databases [37–40].

^1H NMR spectra were manually corrected for phase and baseline deformation using Topspin software (V3.5, Bruker Biospin, Rheinstetten, BW, Germany). The spectra of liver lipid extracts were referenced to the TMS peak (δ , 0 ppm). The spectra ranging from δ 0.5 to δ 5.5 ppm were integrated with an equal width of 0.002 ppm, using the AMIX package (V3.8, Bruker Biospin, Rheinstetten, BW, Germany). Areas of identified lipid peaks were

normalized to wet weight of liver tissues. The relative amount of hepatic lipid for the groups with different treatments was normalized to wild-type control and represents the fold change. Values represent the mean \pm S.E.M.

2.5. Hepatic Fatty Acid Profiling Using Gas Chromatography Coupled Mass Spectrometry (GC-MS)

GC-MS was used as previously described (Zhang, Toxicology, 2020). Briefly, ten milligrams of liver tissue were homogenized with a BeadBlaster Homogenizer (Southern Labware, Cumming, GA, USA) for 90 s (with a 5 s interval for 30 s) in microcentrifuge tubes containing zirconia/silica beads with pre-cooled methanol (HPLC grade). After one 90 s cycle, the liver samples were cooled on ice for 15 min, and this procedure was repeated twice. The liver homogenate was put into glass conical centrifuge tubes and the fatty acids were methylated using a previously reported method with minor modification [41]. An internal standard (1 mg/mL methyl heptadecanoate, 0.5 mg/mL methyl tricosanoate, and 2 mg/mL butylated hydroxytoluene in hexane) was added into each tube containing liver homogenate, followed by the addition of 1 mL methanol/hexane mixture (4:1) and vortexing. Tubes were cooled in liquid nitrogen and then pre-cooled acetyl chloride was added into the mixture slowly. After submersion in liquid nitrogen, the samples were placed at room temperature in the dark for twenty-four hours. Samples were cooled on ice and neutralized by slowly adding 6% K₂CO₃ hexane to the samples, then they were vortexed, and centrifuged to obtain the supernatant. The extraction procedure was repeated three times and combined for each sample. The supernatant in the tubes were then placed in a fume hood to remove the organic solvent. These lipid samples were reconstituted with hexane and transferred to autosampler vials. The fatty acids were quantified using an Agilent 7890A-5975C GC-MS system (Agilent Technologies, Santa Clara, CA, USA) with a previously described procedure [42]. A Supelco 37 Component FAME Mix (Sigma-Aldrich, St Louis, MO, USA) was used to help identify GC-MS peaks.

Detected and identified fatty acids were quantified by comparing integrated peak areas following normalization to the internal standards. The results were expressed as microgram fatty acids per milligram of liver tissue as the mean \pm standard deviation.

2.6. Quantitative Western Blot Analyses of Hepatic 4-Hydroxynonenal (4-HNE)

Approximately fifty milligrams of liver tissue were homogenized with a Dounce tissue grinder in a tube containing RIPA lysis buffer (50 mM Tris base, 150 mM sodium chloride, 1% triton, 0.5% SDS, 0.5% sodium deoxycholate, pH 8.6, and protease inhibitors) on ice. The liver homogenate was centrifuged at 10,000 \times g, 4 °C for 10 min. The supernatant was collected and used for analyses. Quantitative western blotting was performed to measure the level of 4-hydroxynonenal (4-HNE) in the liver as previously described [43]. Briefly, fifty micrograms of protein from each sample were resolved using SDS-PAGE. The gel samples were transferred onto a polyvinylidene difluoride membrane with electroblotting. After blocking the membrane with Tris-buffered saline with 5% milk, the membrane was incubated overnight at 4 °C with an anti-HNE primary antibody (Abcam, ab46545, Waltham, MA, USA) followed by incubation with a biotinylated secondary antibody. Immunoreactive proteins were detected after incubation in [¹²⁵I]-labeled streptavidin using phosphorimaging analysis. Hybridization signals for 4-HNE were normalized to the hybridization signal of the housekeeping protein; lactate dehydrogenase (LDH) (Rockland, Gilbertsville, PA, USA). Independent triplicate samples were used for the analysis of each treatment group.

2.7. Thiobarbituric Acid Reactive Substance (TBARS) Assay

The TBARS assay was performed using a previously reported method with modification [44]. Briefly, twenty milligrams of liver tissue were homogenized with a BeadBlaster Homogenizer (Southern Labware, Cumming, GA, USA) for 90 s (with a 5 s interval for 30 s) in Eppendorf tubes containing zirconia/silica beads with pre-cooled RIPA buffer (with protease inhibitor). After one 90 s cycle, the liver samples were cooled on ice for 15 min,

and this procedure was repeated two more times. The liver homogenate was centrifuged at $3000\times g$, $4\text{ }^{\circ}\text{C}$ for 10 min. The supernatants were transferred to a new tube and then ice cold 10% trichloroacetic acid was added to precipitate proteins. These samples were incubated on ice for 15 min and then centrifuged again at $2200\times g$, $4\text{ }^{\circ}\text{C}$ for 15 min. The supernatant and prepared standards were transferred to new tubes, and an equal volume of 0.67% (*w/v*) thiobarbituric acid was added. These samples were then placed in a boiling water bath for 10 min and cooled down after at room temperature for 30 min. Duplicate samples and standards were transferred into a clear 96-well plate and the absorbance at 532 nm was measured to determine the amount of TBARS in each sample.

2.8. Immunohistochemistry

Formalin-fixed, paraffin-embedded liver tissue sections on slides ($4\text{ }\mu\text{m}$) were placed in a $60\text{ }^{\circ}\text{C}$ oven for 30 min. Slides were deparaffinized, washed in decreasing amounts of ethanol (90–70%), and rehydrated after washing with distilled water and then phosphate buffered saline (PBS). Rehydrated slides were immersed in buffer (10 mM Tris base, 1 mM EDTA (disodium salt), pH 9.0; Cold Spring Harbor Protocols) and subjected to heat-induced epitope retrieval with an IHCWORLD Steamer Set for 50 min. After the slides in buffer cooled down to ambient temperature, they were washed three times with 0.01 M PBS (pH 7.4) for 5 min. Fresh 3% H_2O_2 was applied to each slide section at room temperature for 10 min to inactivate endogenous peroxidase and was washed three times with 0.01 M PBS (pH 7.4) for 5 min each to remove residue of H_2O_2 . Slides were blocked with 5% normal goat serum for 30 min at room temperature and washed three times. After blocking and washing, slides were incubated with either an anti-CD4 antibody (Abcam, ab183685, Waltham, MA, USA), an anti-p21 antibody (Abcam, ab188224, Waltham, MA, USA), or an anti-CDKN2A/p16INK4a antibody (Abcam, ab211542, Waltham, MA, USA) and placed into a humidifier at $4\text{ }^{\circ}\text{C}$ overnight and then into a $37\text{ }^{\circ}\text{C}$ incubator for 45 min. After three washes with 0.01 M PBS (pH 7.4) for 5 min, a horseradish peroxidase-conjugated secondary antibody (Abcam, ab214880, Waltham, MA, USA) was applied to each slide in the humidifier for one hour. After this incubation, the slides were washed three times with 0.01 M PBS (pH 7.4) for 5 min. Processed slides were then incubated with 3,3-diaminobenzidine (DAB) working solution (Vector Laboratories, Newark, CA, USA) at room temperature for one minute and then immersed into tap water to stop the reaction. Slides were sealed with mounting medium (Vector Laboratories, Newark, CA, USA).

Four representative liver tissue slides were examined from each treatment group. For quantification of the cells that stained positive for each protein, ten fields were counted on each slide with a microscope ($100\times$). Regions with a large blood vessel were not examined. The number of positive cells was quantified using ImageJ (Vx, NIH). The number of positive cells from each of the ten fields from four representative mice examined were used to calculate the average number of positive cells per mouse liver section. Relative positive cell number of groups with different treatments was normalized to wild-type control and represents the fold change. Values represent the mean \pm S.E.M.

2.9. Serum $\text{IFN}\gamma$ and $\text{TNF}\alpha$

The concentrations of interferon gamma ($\text{IFN}\gamma$) and tumor necrosis factor alpha ($\text{TNF}\alpha$) in serum were quantified by ELISA assays (BMS609, BMS607HS, Invitrogen, Vienna, Austria). Assays were performed using the manufacturer's recommended protocols.

2.10. Statistical Analyses

The data were analyzed by analysis of variance followed by Tukey's multiple comparisons test (Prism 9.0; GraphPad Software Inc., La Jolla, CA, USA). For all analyses, differences are described when $p \leq 0.05$.

3. Results

To examine the role of mouse or human PPAR α in modulating hepatic lipids, wild-type, *Ppara*-null, or *PPARA*-humanized mice were fed either a control diet or one containing 0.01% GW7647 for either 26 weeks or ~75 weeks (Figure S1). Two different exposure paradigms were used. In the first paradigm, dietary GW7647 was provided to adult mice for either 26 weeks or ~75 weeks (Figure S1a). In the second paradigm, dietary GW7647 was provided to perinatal mice through adulthood for either 26 weeks or ~75 weeks (Figure S1b). Since the focus of these studies is on the effect of constitutive expression/activity of PPAR α and the effect of specific ligand activation of PPAR α , the results are presented in this order, respectively. The effect of age on exposure was also examined by the two different paradigms as the age at termination was 6–12 weeks older in the mice after 26 weeks or ~75 weeks for the “adults only” group compared to the “perinatal + adult” group (Figure S1). Using these approaches allows for comparison with PPAR α -dependent differences in liver carcinogenesis previously reported [13,14].

3.1. Differential Alterations of Hepatic Lipids by Mouse and Human PPAR α

Thirty signal peaks from lipids were identified by NMR in liver samples from both treatment paradigms (Figure S2, Tables S1–S4). Most of these were identified as fatty acids, cholesterol, glycerides, and phospholipids. After 26 weeks, the relative levels of total hepatic fatty acids, triglycerides, unsaturated fatty acids, and polyunsaturated fatty acids were not different between control wild-type or *Ppara*-null mice with either treatment paradigm (Figures 1 and S3). Similarly, after ~75 weeks the relative amount of total hepatic fatty acids, unsaturated fatty acids, and polyunsaturated fatty acids were not different between control wild-type or *Ppara*-null mice with either treatment paradigm (Figures 1 and S3). However, higher hepatic triglycerides were noted in control *Ppara*-null mice compared to control wild-type mice after ~75 weeks in the “adult-only” group (Figure 1). This effect was not noted in the similarly treated “perinatal + adult” group of control *Ppara*-null mice compared to control wild-type mice (Figure S3). The relative amount of total hepatic fatty acids, triglycerides, unsaturated fatty acids, and polyunsaturated fatty acids was higher in control *PPARA*-humanized mice compared to control wild-type mice after 26 or ~75 weeks in the “adult-only” and “perinatal + adult” groups (Figures 1 and S3).

No differences in total hepatic omega 3 fatty acids or docosahexaenoic acid were noted between control or *Ppara*-null mice from either treatment paradigm (Figure S4). The average concentration of linoleic acid in the liver was higher in control *Ppara*-null mice and control *PPARA*-humanized mice compared to wild-type controls after 26 weeks or ~75 weeks in the “perinatal + adult” group (Figure 2c,d). Higher liver linoleic acid was only noted in control *Ppara*-null mice after ~75 weeks in the “adult only” group (Figure 2a,b). The average concentration of linoleic acid in the liver was higher in control *PPARA*-humanized mice compared to wild-type control for both treatment paradigms (Figure 2). The higher hepatic concentration of linoleic acid in control *Ppara*-null and control *PPARA*-humanized mice detected by NMR after ~75 weeks was confirmed with GC/MS (Figure S5). Interestingly, the average hepatic concentration of linoleic acid was higher in both *Ppara*-null and control *PPARA*-humanized mice compared to control wild-type mice after 26 or ~75 weeks for both treatment paradigms (Figure 2).

3.2. Activation of Mouse or Human PPAR α with a High Affinity Ligand Differentially Alters Hepatic Lipids

Ligand activation of PPAR α with GW7647 in wild-type mice for 26 weeks and ~75 weeks altered the amount of total cholesterol, esterified cholesterol, free cholesterol, total fatty acids, monoglycerides, phosphatidylethanolamine, sphingomyelin, phosphatidylcholine, total phospholipids, and diglycerol phosphate in the liver (Tables S1–S4). Ligand activation of PPAR α with GW7647 for 26 weeks in wild-type mice caused an increase in hepatic fatty acids, triglycerides, and unsaturated fatty acids but no changes in polyunsaturated fatty acids, in both “adult only” and “perinatal + adult” groups (Figures 1 and S3). This effect after 26 weeks was diminished in

similarly treated *Ppara*-null mice in both the “adult only” and “perinatal + adult” groups (Figures 1 and S3). Ligand activation of PPAR α with GW7647 for 26 weeks in *PPARA*-humanized mice did not cause an increase in hepatic fatty acids, triglycerides, unsaturated fatty acids, or polyunsaturated fatty acids in the “perinatal + adult” group compared to wild-type controls (Figure S3). However, it is important to note that in *PPARA*-humanized mice administered with GW7647 for 26 weeks, hepatic fatty acids, triglycerides, unsaturated fatty acids, or polyunsaturated fatty acids in the “adult only” control and ligand-treated groups were high compared to wild-type control but had similar levels as those observed after ligand activation of PPAR α in wild-type mice (Figure 1). A similar trend was observed in *PPARA*-humanized mice administered GW7647 for 26 weeks in the “perinatal + adult” group compared to wild-type controls (Figure S3). After ~75 weeks, no ligand-dependent increases in hepatic fatty acids, triglycerides, and unsaturated fatty acids were observed in any genotype, in either treatment paradigms (Figures 1 and S3). It is important to note that compared to wild-type controls, liver triglycerides, unsaturated fatty acids, and polyunsaturated fatty acids were relatively higher in *PPARA*-humanized mice after ~75 weeks of ligand activation of PPAR α by GW7647 in the “adult only” group, but not in the “perinatal + adult” group (Figures 1 and S3).

Ligand activation of PPAR α with GW7647 in wild-type mice caused no change in total hepatic omega 3 fatty acids or docosahexaenoic acid compared to respective wild-type control with either treatment paradigm (Figure S4). Notably, liver linoleic acid was higher in wild-type mice after 26 weeks of dietary GW7647 (Figure 2a,c), but not after ~75 weeks, with both treatment paradigms (Figure 2b,d). In *Ppara*-null mice, administration of dietary GW7647 did not affect liver omega 3 fatty acid concentrations compared to controls after 26 or ~75 weeks in both the “adult only” group and “perinatal + adult” group (Figure S4). However, administration of dietary GW7647 to *Ppara*-null mice for either 26 or ~75 weeks resulted in higher liver docosahexaenoic acid in the “perinatal + adult” group compared to both wild-type and *Ppara*-null controls (Figure S4); this effect was not observed in the similarly treated “adult-only” group (Figure S4). Interestingly, dietary administration of GW7647 in *Ppara*-null mice also resulted in higher liver linoleic acid compared to both wild-type and *Ppara*-null controls, but this effect was only observed in the “perinatal + adult” group (Figure 2c), and not in the “adult only” group (Figure 2a). Administration of dietary GW7647 to *PPARA*-humanized mice for 26 weeks or ~75 weeks caused no change in liver omega 3 fatty acids or docosahexaenoic acid in the “adult only” and “perinatal + adult” groups compared to control (Figure S4). It is also important to note that the average level of liver omega 3 fatty acids or docosahexaenoic acid was higher in the “adult only” groups compared to wild-type control but dietary administration of GW7647 did not further alter these levels (Figure S4). Similarly, while the average concentration of hepatic linoleic acid was not affected by GW7647, liver linoleic acid levels were higher after 26 weeks or ~75 weeks in *PPARA*-humanized mice in the “adult only” and “perinatal + adult” groups compared to control (Figure 2). The NMR analyses described above were confirmed with GC/MS (Figure S5). The average concentrations of linoleic acid in liver were not altered by ligand activation of PPAR α with GW7647 in wild-type mice ~75 weeks for both the “adult only” and “perinatal + adult” groups (Figures 2 and S5). By contrast, the average concentration of hepatic linoleic acid was markedly higher in both the control and GW7647-treated *Ppara*-null or *PPARA*-humanized mice compared to control and GW7647-treated wild-type mice after ~75 weeks (Figures 2 and S5).

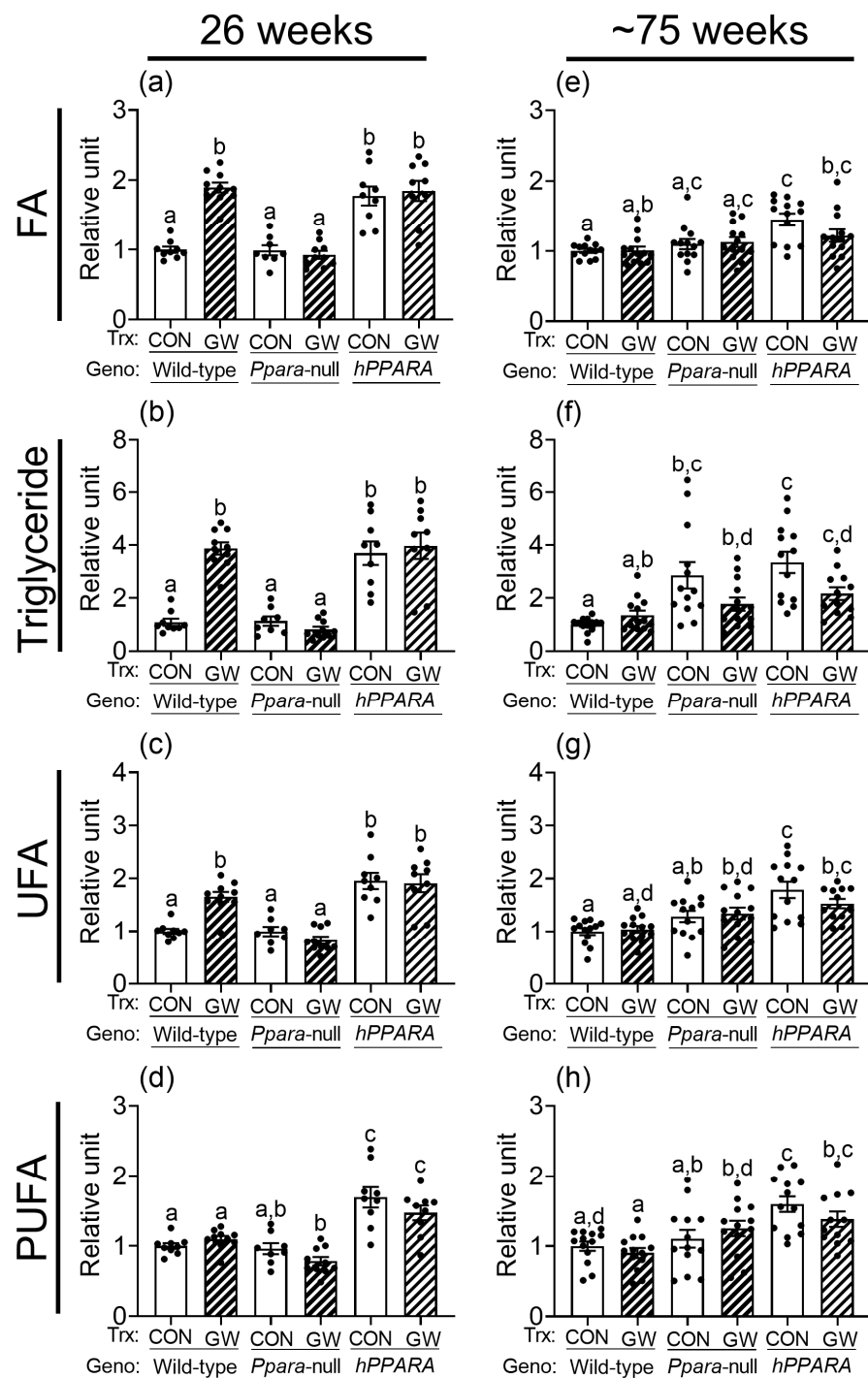


Figure 1. Relative levels of fatty acids (a,e), triglycerides (b,f), unsaturated fatty acids (UFA; c,g), or polyunsaturated fatty acids (PUFA; d,h) in lipophilic liver extracts from “adult only” groups of wild-type, *Ppara*-null, or *PPARA*-humanized mice with or without ligand activation of *PPAR* α after 26 weeks (a–d) or ~75 weeks (e–h). Fatty acid residues ($R-CH_3$), triglycerides (C_1H and C_3H of glycerol), unsaturated fatty acid (UFA) residues ($-CH=CH-$), and polyunsaturated fatty acid (PUFA) residues ($-CH=CH-CH_2-(CH=CH-CH_2)_n$). CON, control mouse group; GW, GW7647-treated mouse group. The relative average amount of lipids in the liver of mice with different treatments was normalized to wild-type control and represents the fold change. Values represent the mean \pm S.E.M. Groups with different superscript letters are significantly different at $p \leq 0.05$. (One-way ANOVA followed by Tukey’s multiple comparisons test).

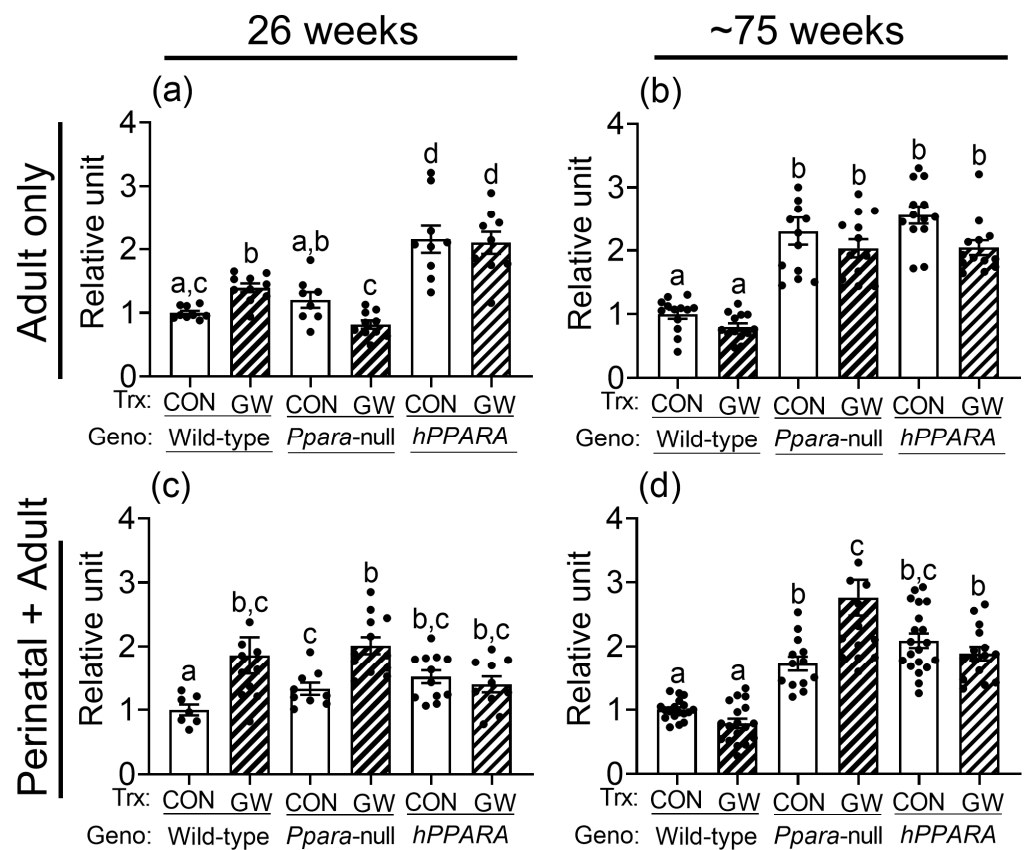


Figure 2. NMR detection of linoleic acid in lipophilic liver extracts from both “adult only” and “perinatal + adult” groups of wild-type, *Ppara*-null, or *PPARA*-humanized mice with or without ligand activation of PPAR α . NMR was used to detect linoleic acid after either 26 weeks or ~75 weeks in “adult only” (a,b) or “perinatal + adult” (c,d) groups. Relative amount of lipids in livers was normalized to wild-type control and represents the fold change. Values represent the mean \pm S.E.M. Groups with different superscript letters are significantly different at $p \leq 0.05$. (One-way ANOVA followed by Tukey’s multiple comparisons test).

3.3. Increased Lipid Peroxidation Is Not Associated with Hepatic Fatty Acid Accumulation

Reactive oxygen species produced by lipid peroxidation can damage membrane structure/function, contribute to mutagenesis/carcinogenesis, and ultimately lead to cell death. To determine whether increased oxidative stress results from the observed accumulation of hepatic linoleic acid in *Ppara*-null or *PPARA*-humanized mice, 4-hydroxy-2-nonenal (4-HNE) and malondialdehyde (MDA) were measured (the main metabolites produced by peroxidation of linoleic acid). The average level of liver 4-HNE was not different between any genotype or treatment group, with either “adult only” and “perinatal + adult” groups compared to wild-type control (Figure 3a,b). In contrast, the hepatic concentration of MDA was lower in both control in *Ppara*-null or *PPARA*-humanized mice in either “adult only” and “perinatal + adult” groups compared to control wild-type mice (Figure 3c,d). Ligand activation of PPAR α with GW7647 in wild-type mice in the “adult only” or “perinatal + adult” groups caused a decrease in liver MDA concentration compared to control (Figure 3c,d). This effect was not observed in similarly treated *Ppara*-null or *PPARA*-humanized mice with either treatment paradigm (Figure 3c,d).

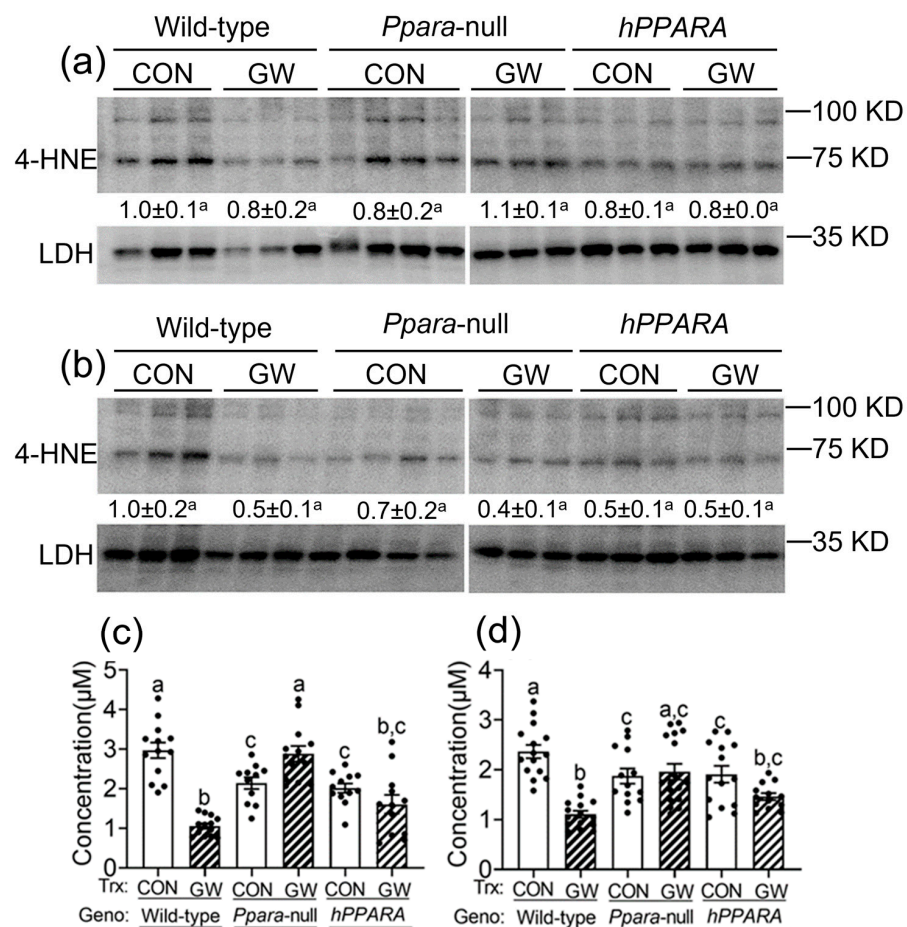


Figure 3. Assessment of oxidative stress in liver from “adult only” and “perinatal + adult” groups of wild-type, *Ppara*-null, or *PPARA*-humanized mice with or without ligand activation of PPAR α . Both 4-hydroxynonenal (4-HNE, **a,b**) and malondialdehyde (MDA, **c,d**) levels in liver were measured after ~75 weeks in mice from both treatment paradigms. **a** and **c**, “adult only”; **b** and **d**, “perinatal + adult” groups. For the 4-HNE Western blot analyses (**a,b**) the relative amount of 4-HNE was normalized to the signal for lactate dehydrogenase (LDH) for wild-type control and represents the fold change. All values represent the mean \pm S.E.M. Groups with different superscript letters are significantly different at $p \leq 0.05$. (One-way ANOVA followed by Tukey’s multiple comparisons test).

3.4. Hepatic CD4⁺ T Lymphocytes Is Inversely Correlated with Linoleic Acid Accumulation

The concentration of linoleic acid was higher in the liver of all the *Ppara*-null and humanized-*PPARA* mice with and without ligand activation of PPAR α with GW7647. As previous studies showed that higher hepatic linoleic acid causes loss of CD4⁺ T lymphocytes and promotes hepatocarcinogenesis [45–47], the relative abundance of CD4⁺ T lymphocytes was measured by immunohistochemistry. In the “adult only” and “perinatal + adult” groups of control wild-type mice there were more hepatic CD4⁺ T lymphocytes after ~75 weeks compared to that observed after 26 weeks in their respective control (Figure 4a). In the “adult only” and “perinatal + adult” groups of control *Ppara*-null and *PPARA*-humanized mice there were also more CD4⁺ T lymphocytes in the liver after ~75 weeks compared to that observed after 26 weeks in their respective control (Figure 4). However, by contrast, the average number of liver CD4⁺ T lymphocytes in the “adult only” and “perinatal + adult” groups of control *Ppara*-null and control *PPARA*-humanized mice was lower compared to control wild-type mice from both treatment paradigms (Figure 4), particularly after ~75 weeks. Ligand activation of PPAR α with GW7647 in wild-type mice in the “adult only” group caused a decrease in hepatic CD4⁺ T lymphocytes after 26 or ~75 weeks compared to the respective control group (Figure 4). Similarly, ligand activation

of PPAR α with GW7647 in wild-type mice in the “perinatal + adult” caused a decrease in hepatic CD4 $^+$ T lymphocytes after ~75 weeks (but not after 26 weeks) compared to the respective control (Figure 4). This decrease in liver CD4 $^+$ T lymphocytes by ligand activation of PPAR α with GW7647 after 26 or ~75 weeks was not observed in either *Ppara*-null and *PPARA*-humanized mice (Figure 4). The lower number of liver CD4 $^+$ T cells correlated with higher concentrations of liver linoleic acid (Figure S6).

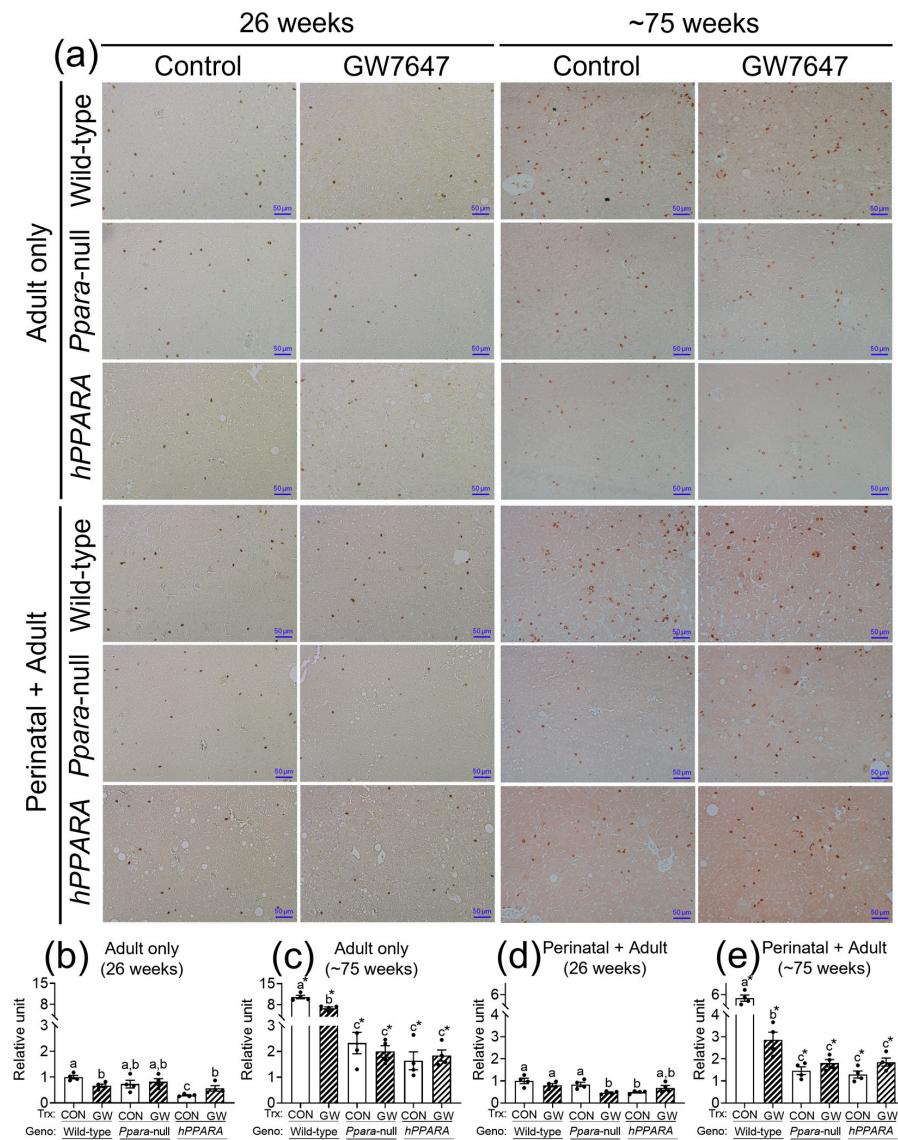


Figure 4. Representative photomicrographs of immunohistochemical detection of CD4 $^+$ T cells (a) in liver from “adult only” and “perinatal + adult” groups of wild-type, *Ppara*-null, or *PPARA*-humanized mice with or without ligand activation of PPAR α with GW7647 after 26 weeks (left panels) or ~75 weeks (right panels). The relative amount of CD4 $^+$ T cells in liver was normalized to wild-type control and represents the fold change (b–e). Values represent the mean \pm S.E.M. Groups with different superscript letters are significantly different at $p \leq 0.05$. * significantly different at $p \leq 0.05$ for the mouse treatment groups after 26 weeks (b,d) compared to the mouse treatment groups at ~75 weeks (c,e), respectively. (One-way ANOVA followed by Tukey’s multiple comparisons test).

3.5. Senescent Hepatocytes Increase in Liver of GW7647-Treated Mice

CD4 $^+$ T lymphocytes have an important role in clearing senescent hepatocytes. Thus, we examined senescent markers to determine if linoleic acid associated liver CD4 $^+$ T lymphocyte loss influences senescence of hepatocytes. In the “adult only” and “perinatal + adult” groups

of control wild-type mice there were few hepatocytes expressing P16 or P21 after 26 or ~75 weeks (Figures 5 and 6). By contrast, in the “adult only” and “perinatal + adult” groups of control *Ppara*-null and *PPARA*-humanized mice there were more hepatocytes expressing P16 and P21 after 26 or ~75 weeks compared to wild-type controls (Figures 5 and 6). Ligand activation of PPAR α with GW7647 in wild-type mice in the “adult only” and “perinatal + adult” groups caused an increase in P16-positive and P21-positive hepatocytes after 26 or ~75 weeks compared to the respective control group (Figures 5 and 6). Interestingly, administration of GW7647 did not further influence the number of P16-positive or P21-positive hepatocytes in the “adult only” and “perinatal + adult” groups of *Ppara*-null and *PPARA*-humanized mice whose expression of P16 and P21 were higher as compared to control wild-type mice (Figures 5 and 6).

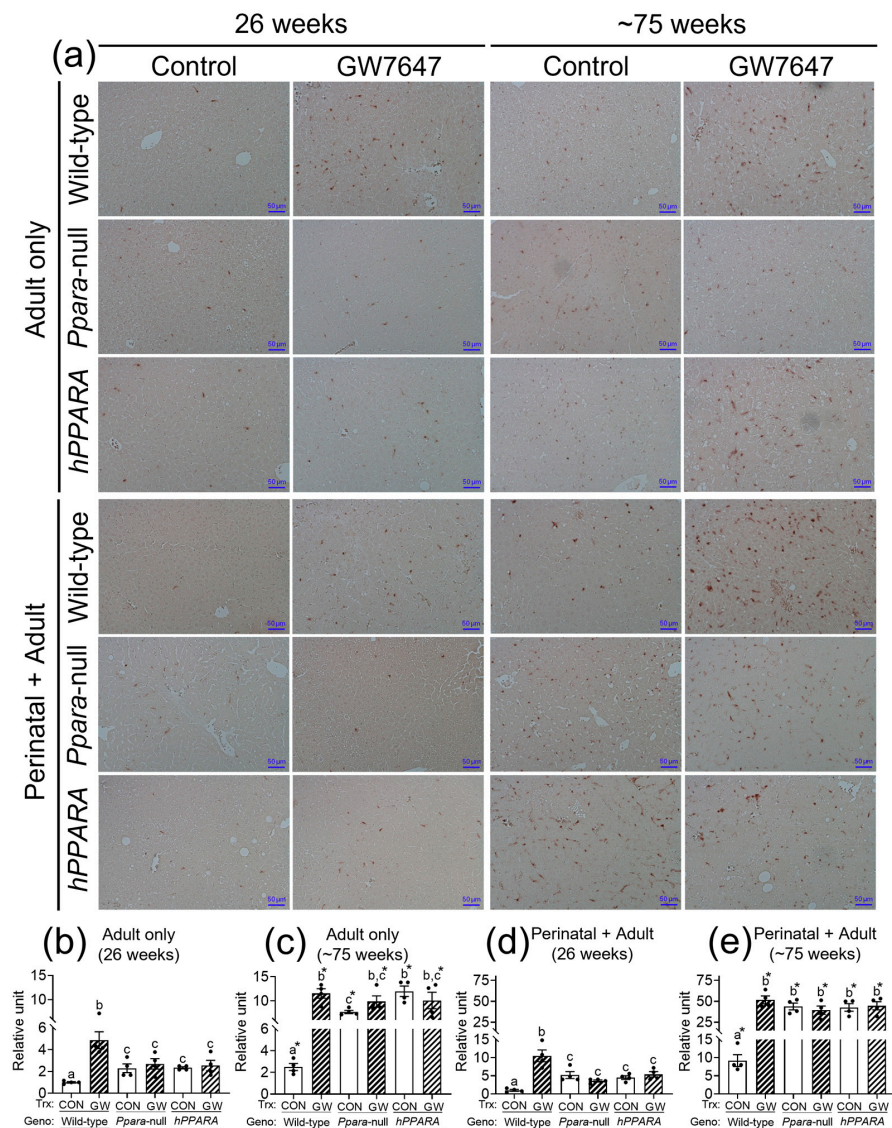


Figure 5. Representative photomicrographs of immunohistochemical detection of P16 (a) in liver from “adult only” and “perinatal + adult” groups of wild-type, *Ppara*-null, or *PPARA*-humanized mice with or without ligand activation of PPAR α with GW7647 after 26 weeks (left panels) or ~75 weeks (right panels). The relative amount of P16-positive cells in liver was normalized to wild-type control and represents the fold change (b–e). Values represent the mean \pm S.E.M. Groups with different superscript letters are significantly different at $p \leq 0.05$. * significantly different at $p \leq 0.05$ for the mouse treatment groups after 26 weeks (b,d) compared to the mouse treatment groups at ~75 weeks (c,e), respectively. (One-way ANOVA followed by Tukey’s multiple comparisons test).

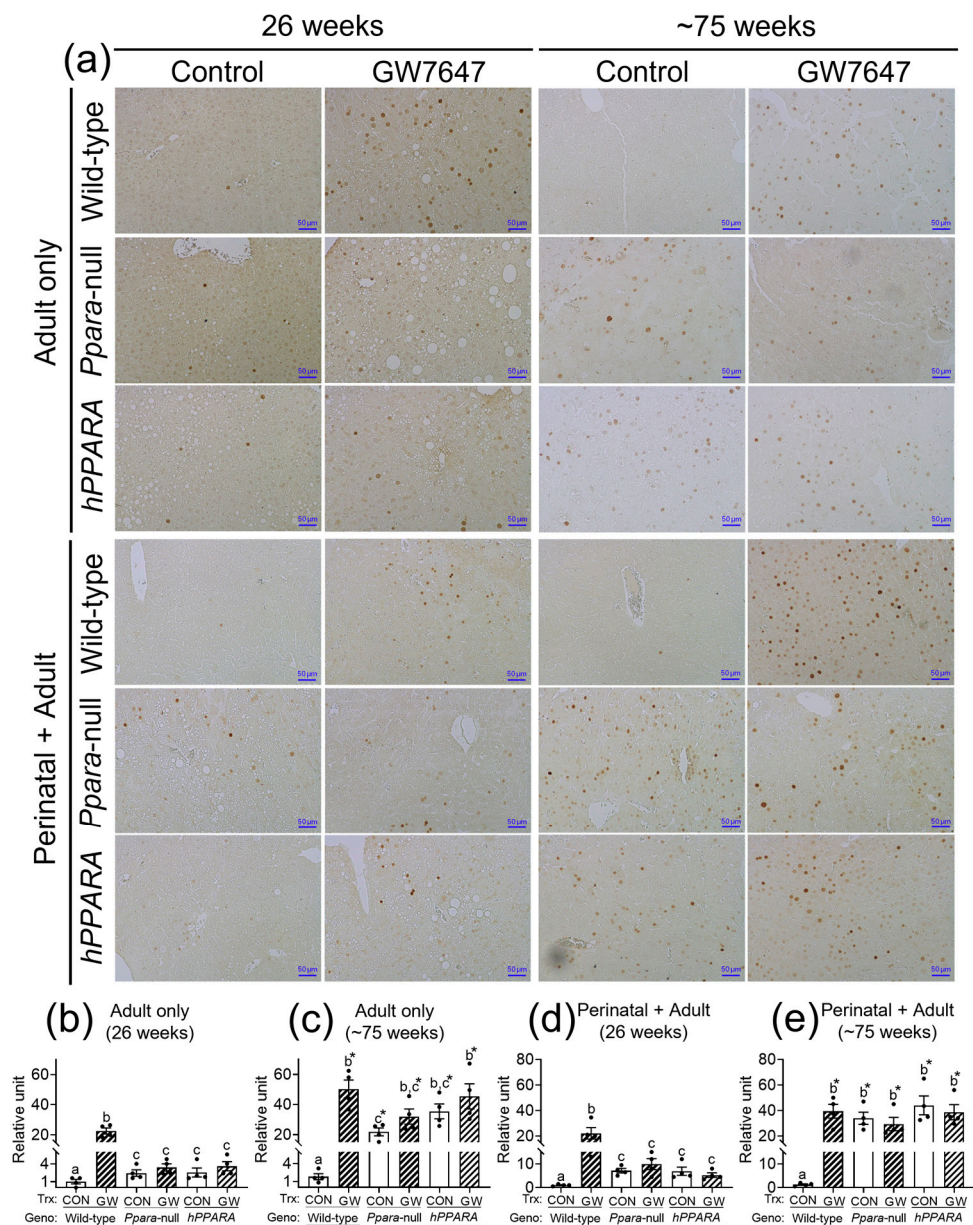


Figure 6. Representative photomicrographs of immunohistochemical detection of P21 (a) in liver from “adult only” and “perinatal + adult” groups of wild-type, *Ppara*-null, or *PPARA*-humanized mice with or without ligand activation of *PPAR* α with GW7647 after 26 weeks (left panels) or ~75 weeks (right panels). Relative amount of P21-positive cells in liver was normalized to wild-type control and represents the fold change (b–e). Values represent the mean \pm S.E.M. Groups with different superscript letters are significantly different at $p \leq 0.05$. * significantly different at $p \leq 0.05$ for the mouse treatment groups after 26 weeks (b,d) compared to the mouse treatment groups at ~75 weeks (c,e), respectively. (One-way ANOVA followed by Tukey’s multiple comparisons test).

3.6. Lower Liver $CD4^+$ T Cells Are Associated with Reduced Production of Serum Cytokines

Since $CD4^+$ T cells regulate the production of gamma interferon (IFN- γ) and tumor necrosis factor alpha (TNF- α), which have important roles in immune surveillance, these were measured in serum. Serum IFN- γ was similar between control wild-type, *Ppara*-null, and *PPARA*-humanized mice in both the “adult only” and “perinatal + adult” groups of control mice after 26 weeks (Figure 7). Serum IFN γ was lower in *Ppara*-null and *PPARA*-humanized mice in both the “adult only” and “perinatal + adult” groups compared to control wild-type mice after ~75 weeks (Figure 7). Ligand activation of *PPAR* α with GW7647 did not influence

serum IFN γ in either the “adult only” and “perinatal + adult” groups compared to wild-type controls after 26 or ~75 weeks (Figure 7). Serum TNF α was similar between control wild-type and *Ppara*-null mice in the “adult only” and “perinatal + adult” groups of mice after 26 weeks (Figure 7). By contrast, serum TNF α was lower in control *PPARA*-humanized mice compared to control wild-type mice in the “adult only” and “perinatal + adult” groups after 26 weeks (Figure 7). Serum TNF α was lower in control *Ppara*-null and *PPARA*-humanized mice compared to control wild-type mice in the “adult only” and “perinatal + adult” groups after ~75 weeks (Figure 7). Ligand activation of PPAR α with GW7647 in wild-type mice decreased serum TNF α in both the “adult only” and “perinatal + adult” groups compared to wild-type controls after 26 or ~75 weeks (Figure 7). This effect did not occur in similarly treated *Ppara*-null mice in the “adult only” groups (Figure 7). Administration of GW7647 caused lower serum TNF α in *Ppara*-null mice in the “perinatal + adult” group, but this effect was not observed after ~75 weeks (Figure 7). Administration of GW7647 to *PPARA*-humanized mice had no effect on serum TNF α in both the “adult only” and “perinatal + adult” groups compared to controls after either 26 or ~75 weeks (Figure 7).

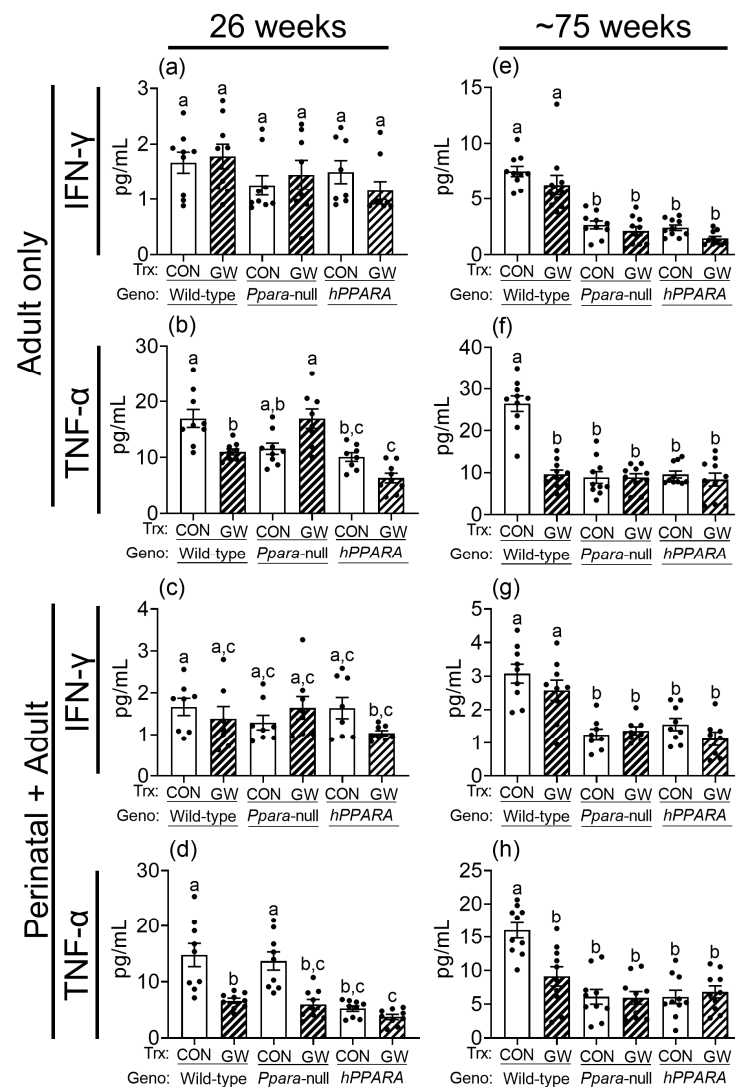


Figure 7. Average serum concentration of IFN γ (a,c,e,g), TNF α (b,d,f,h) in “adult only” and “perinatal + adult” groups of wild-type, *Ppara*-null, or *PPARA*-humanized mice with or without ligand activation of PPAR α with GW7647 after 26 weeks (left panels) or ~75 weeks (right panels). Values represent the mean \pm S.E.M. Groups with different superscript letters are significantly different at $p \leq 0.05$. (One-way ANOVA followed by Tukey’s multiple comparisons test).

4. Discussion

Results from these studies extend our understanding of the role of metabolism in liver cancer. The use of wild-type, *Ppara*-null, or *PPARA*-humanized mice, coupled with chronic ligand activation of PPAR α administered using different ages of mice (“adult only” and “perinatal + adult”) to initiate ligand activation of PPAR α provided a platform to critically examine: (1) how liver metabolism adapts during PPAR α agonist-induced liver carcinogenesis; (2) whether mouse or human PPAR α modulate liver metabolism differentially during PPAR α agonist-induced liver carcinogenesis; and (3) whether aging influenced either liver metabolism and/or species differences in PPAR α agonist-induced liver carcinogenesis.

Chronic ligand activation of PPAR α causes liver cancer in rodents [48]. However, *Ppara*-null mice are resistant to PPAR α agonist-induced liver cancer demonstrating that PPAR α mediates hepatocarcinogenesis resulting from exposure to these non-genotoxic rodent carcinogens [13–17]. Diminished liver carcinogenesis has also been observed in *PPARA*-humanized mice after chronic administration of PPAR α agonists demonstrating the mechanism of species differences in liver cancer between rodents and humans [13,14,16]. These observations coupled with a larger body of evidence indicate that rodents can develop liver cancer after chronic administration of PPAR α agonist whereas humans do not [5,9–11,21–23,49,50]. Results from the present studies show that PPAR α -dependent effects increase fatty acids, triglycerides, and monounsaturated fatty acids in the liver metabolome in wild-type mice, and are not found in similarly treated *Ppara*-null mice. Interestingly, this is consistent with the finding that ligand activation of PPAR α caused a small receptor-dependent increase in the concentration of hepatic linoleic acid after 26 weeks, but this change was not noted after ~75 weeks. Whether this change is causally related to, or associated with, PPAR α agonist-induced hepatocarcinogenesis noted in the previous studies [13,14] is uncertain. As these PPAR α -dependent effects were the same in both “adult only” and “perinatal + adult” groups compared to control suggests that this effect is not impacted by aging. However, it is worth noting that changes in liver linoleic acid were also noted in older control and GW7647-treated *Ppara*-null and *PPARA*-humanized mice, and the observed changes in liver linoleic acid were different than those observed in wild-type mice.

While there is strong evidence that PPAR α is required to mediate liver carcinogenesis caused by chronic ligand activation of PPAR α in rodents, there is equally convincing evidence that humans do not develop liver cancer following administration of PPAR α agonists (reviewed in [5,9–11,21,22,49,50]). This is based on different types of studies ranging from retrospective and prospective studies showing no change in liver cancer in humans treated with PPAR α ligands (e.g., fibrate drugs), to preclinical studies showing that *Ppara*-null and *PPARA*-humanized mice are refractory to liver carcinogenesis after long-term administration of PPAR α agonists [5,9,13–16,21,22], and lack of increased proliferation of human hepatocytes in chimeric humanized mice [23]. Indeed, there is a consensus that ligand activation of PPAR α can cause liver carcinogenesis in rodents but ligand activation of PPAR α in humans does not [5,9,21,22]. However, it is critical to note that both *Ppara*-null and *PPARA*-humanized mice both develop liver tumors with or without administration of PPAR α agonists but that the observed phenotype is different than that found in wild-type mice [13–15,24]. The present studies provide new evidence that may explain how liver carcinogenesis found in aged *Ppara*-null and *PPARA*-humanized mice is different than that which occurs by ligand activation of PPAR α . In the *Ppara*-null and *PPARA*-humanized mice, there is an accumulation of hepatocellular lipids, leading to macrosteatosis (a form of hepatocellular toxicity) with consequent increased cellular proliferation and an increased risk of hepatocellular cancer [13,14,21,51]. This accumulation of fat is a consequence of the altered lipid metabolism occurring in the absence of PPAR α expression.

It is well-established that PPAR α regulates the expression of key gene products involved in metabolism including fatty acid binding, mitochondrial and peroxisomal fatty acid oxidation, ketogenesis, triglyceride turnover, gluconeogenesis, and bile synthesis/secretion [52,53].

Additionally, expression of PPAR α is relatively high in the liver because lipids are extensively metabolized in this tissue [52,53]. This is consistent with the reduced constitutive expression of mitochondrial fatty acid metabolizing enzymes in the liver and accompanies an increase in serum and liver lipids in *Ppara*-null mice compared to wild-type controls [25,54]. Results from the present analyses demonstrated enhanced hepatic lipid accumulation with aging, which is similar to the phenotype noted in other studies in both *Ppara*-null and *PPARA*-humanized mice [13,14]. Accumulation of intracellular lipids can be oxidized to produce peroxidation products that can be mutagenic and carcinogenic [55]. Since no changes in hepatic 4-HNE and MDA concentration were detected in either *Ppara*-null and *PPARA*-humanized mice, this suggests that peroxidation of accumulated lipids does not appear to contribute to the mechanisms that cause liver tumors in *Ppara*-null and *PPARA*-humanized mice.

Results from these studies demonstrate for the first time that the concentration of linoleic acid is markedly higher in the liver of relatively older *Ppara*-null and *PPARA*-humanized mice compared to older wild-type mice. The higher concentration of liver linoleic acid was observed in both “adult only” and “perinatal + adult” groups compared to controls, and this effect was greatest after ~75 weeks. This effect is likely due in part to the aging of *Ppara*-null and *PPARA*-humanized mice compared to wild-type mice. Initiation of ligand administration during perinatal development of *Ppara*-null and *PPARA*-humanized mice (“perinatal + adult” groups) caused similar changes in hepatic linoleic acid concentration as those observed in the “adult only” groups.

High levels of hepatic linoleic acid can selectively cause CD4⁺ T cell loss in the liver [45,47,56], and the antitumor T-cell response in liver carcinogenesis can be inhibited by high dietary linoleic acid [46]. Results from the present studies demonstrate a decrease in the number of hepatic CD4⁺ T cells in *Ppara*-null and *PPARA*-humanized mice that inversely correlated with the concentration of linoleic acid in the liver. Administration of GW7647 did not further impact this phenotype in either *Ppara*-null and *PPARA*-humanized mice, in both the “adult only” and “perinatal + adult” groups of mice. This suggests that the higher liver linoleic acid in *Ppara*-null and *PPARA*-humanized mice may cause a decrease in CD4⁺ T cells, consistent with past studies [45,47,56]. Furthermore, since CD4⁺ T cells are critical for tumor surveillance and suppression, this indicates that reduced CD4⁺ T cells could lead to abnormal cell signaling that causes liver tumorigenesis [56–59].

IFN γ and TNF α are known to mediate some antitumor effects of CD4⁺ T cells [60–62]. Thus, it is of interest to note that the serum concentrations of IFN γ and TNF α are significantly lower in *Ppara*-null and *PPARA*-humanized mice compared to wild-type controls consistent with the lower levels of CD4⁺ T cells found in these mice. These data collectively suggest that higher liver linoleic acid may cause CD4⁺ T cell loss and reduced expression of IFN γ and TNF α in the liver of *Ppara*-null and *PPARA*-humanized mice, and this mechanism may contribute to the age-related hepatocarcinogenesis observed in these mice. Administration of GW7647 did not further affect serum concentrations of IFN γ and TNF α compared to control *Ppara*-null and *PPARA*-humanized mice in both the “adult only” and “perinatal + adult” groups of mice after ~75 weeks. Combined, these data suggest that ligand activation of mouse PPAR α is associated with lower CD4⁺ T cells in wild-type mice, and that this may contribute to reduced expression of TNF α (but not IFN γ) and less antitumor immune function in the liver. By contrast, genetic silencing of PPAR α expression causes larger increases in liver linoleic acid over time, and this phenotype is accompanied with a reduced CD4⁺ T cell number in the liver, and lower serum IFN γ and TNF α compared to wild-type controls. Interestingly, this indicates that this phenotype observed in the absence of PPAR α expression (*Ppara*-null mice), differs from that found in response to ligand activation of PPAR α in wild-type mice. Moreover, the administration of GW7647 did not markedly alter this phenotype demonstrating that this ligand does not activate PPAR α in *Ppara*-null mice. *PPARA*-humanized mice exhibit a similar phenotype to *Ppara*-null mice with higher liver linoleic acid over time accompanied with a reduced hepatic CD4⁺ T cell number and lower serum IFN γ and TNF α compared to wild-type controls, a phenotype

not further impacted by administration of GW7647. Since GW7647 is a potent human PPAR α agonist, these observations suggest that there is a species difference in the ability of the human PPAR α to modulate the same pathways as the mouse PPAR α .

CD4⁺ T cells have important roles in tumorigenesis because they help with turnover of senescent cells [57,63–65]. Aging is associated with an increase in senescence because of less surveillance of tumors provided by CD4⁺ T cells [57,63–65]. Based on the expression of P16 and P21, the present studies suggest that ligand activation caused a mouse PPAR α -dependent increase in senescent liver cells. This effect may represent a new mechanism that contributes to PPAR α agonist-induced mouse liver carcinogenesis mediated by enhanced hepatocyte proliferation accompanied with accumulation of more senescent liver cells. Importantly, the changes in this signaling in wild-type mice are markedly different than those found in *Ppara*-null and *PPARA*-humanized mice. The number of senescent cells in control *Ppara*-null and *PPARA*-humanized mouse liver was higher compared to control wild-type, and this effect was greater in older *Ppara*-null and *PPARA*-humanized mice compared to control wild-type mice. The increase in senescent cells in *Ppara*-null and *PPARA*-humanized mice could be due to the impaired function of CD4⁺ T cells as a result of aging. The changes in liver cell senescence in relatively older *Ppara*-null and *PPARA*-humanized mice were comparable to liver cell senescence in wild-type mice observed in response to ligand activation of PPAR α , independent of GW7647 administration and age. As cellular senescence is one mechanism involved in the regulation and suppression of tumor cells [64], the differential increase in senescent liver cells could contribute to the mechanisms mediating liver carcinogenesis observed in older *Ppara*-null and *PPARA*-humanized mouse liver [66,67]. The role of immunosurveillance activities of CD4⁺ T cells is best characterized in viral-dependent cancer models [56–59]. Thus, since hepatic macrosteatosis can cause hepatocyte cytotoxicity, enhanced inflammation, and regenerative proliferation, it remains possible that the reduction in CD4⁺ T cells noted is secondary to hepatic macrosteatosis. Alternatively, the changes in liver metabolism noted in the present studies may be influenced/reflected by hepatic enzymes that can also interact with other pathways (e.g., immune system and cellular metabolism) and contribute to disease progression [68].

5. Conclusions

Collectively, these findings indicate that PPAR α agonists cause liver cancer in mice through a mechanism that is associated with PPAR α -dependent modulation of lipid metabolism including modest accumulation of linoleic acid, reduced hepatic CD4⁺ T cells, increased cellular senescence, and lowered serum cytokines. These studies also demonstrate a novel, alternative mechanism for carcinogenesis related to the accumulation of hepatic linoleic acid in *Ppara*-null and *PPARA*-humanized mice, an effect related to the loss of the PPAR α regulation of lipid metabolism in hepatocytes. While no loss-of-function mutations of *PPARA* have been reported, results from these studies suggest that mutant, less functional PPAR α could be a risk factor for liver cancer due to dysfunctional regulation of linoleic acid metabolism, reduced CD4⁺ T cell presence and function, and increased hepatocyte senescence. Results from these studies also indicate that liver tumors found in older *Ppara*-null and *PPARA*-humanized mice are mediated by the accumulation of liver linoleic acid that impairs CD4⁺ T cells in the liver and causes age-related accumulation of senescent liver cells. *Ppara*-null and *PPARA*-humanized mouse models remain valuable models to study the mechanisms of PPAR α -agonist induced hepatocarcinogenesis, but background liver tumorigenesis must be factored into the interpretation of the results of such studies.

Supplementary Materials: The following supporting information can be downloaded at: <https://www.mdpi.com/article/10.3390/metabo13080936/s1>, Figure S1: Schematic of two treatment paradigms; Figure S2: Representative 600 MHz ¹H-NMR spectrum of lipophilic mouse liver extract; Figure S3: Relative levels of fatty acids (a and e), triglycerides (b and f), unsaturated fatty acids (UFA; c and g), or polyunsaturated fatty acids (PUFA; d and h) in lipophilic liver extracts from “perinatal + adult”

groups of wild-type, *Ppara*-null or *PPARA*-humanized mice with or without ligand activation of PPAR α after 26 weeks (a–d) or ~75 weeks (e–h); Figure S4: Relative average concentration of ω -3 fatty acids (a, c, e, g) or docosahexaenoic acid (DHA; b, d, f, h), in lipophilic liver extracts from “adult only” and “perinatal + adult” groups of wild-type, *Ppara*-null, or *PPARA*-humanized mice with or without ligand activation of PPAR α with GW7647 after 26 weeks (left panels) or ~75 weeks (right panels); Figure S5: Determining liver linoleic acid with GC-MS in liver from “adult only” (a) and “perinatal + adult” (b) groups of wild-type, *Ppara*-null, or *PPARA*-humanized mice with or without ligand activation of PPAR α after ~75 weeks; Figure S6: Correlation between liver linoleic acid concentration and the number of CD4⁺ T cells in liver of in “adult only” (upper panels) and “perinatal + adult” (lower panels) groups of wild-type, *Ppara*-null, or *PPARA*-humanized mice after 26 weeks (left panels) or ~75 weeks (right panels); Tables S1–S4: Summary of other significantly changed liver lipids in mice of groups.

Author Contributions: A.D.P., J.M.P. and F.J.G. designed the experiments, supervised the studies, and contributed to the financial support of the studies. X.Z. undertook and completed the analysis, performed data processing, generated the figures, and wrote the manuscript. Q.L. performed some GC-MS experiments and data processing. A.K.S. and S.G.A. synthesized GW7647. S.M.C. provided feedback on the study design, analysis, and interpretation of data. All authors contributed to writing and editing the manuscript. All authors have read and agreed to the published version of the manuscript.

Funding: This work was supported in part by the USDA National Institute of Food and Agriculture and Hatch Appropriations under PEN04772.

Institutional Review Board Statement: The study was approved by the Pennsylvania State University Institutional Animal Care and Use Committee (IACUC31363, 17 May 2011).

Informed Consent Statement: Not applicable.

Data Availability Statement: The data presented in this study are available on request from the corresponding author. The data are not publicly available due to the author’s preference.

Acknowledgments: The authors gratefully acknowledge the Penn State Cancer Institute Organic Synthesis Shared Resource for the synthesis of some of the GW7647 used and the Metabolomics Shared Resource used for analyses in these studies.

Conflicts of Interest: All authors state that there are no perceived conflict of interest.

References

1. Berger, J.; Moller, D.E. The mechanisms of action of PPARs. *Annu. Rev. Med.* **2002**, *53*, 409–435. [[CrossRef](#)]
2. Shearer, B.G.; Hoekstra, W.J. Recent advances in peroxisome proliferator-activated receptor science. *Curr. Med. Chem.* **2003**, *10*, 267–280. [[CrossRef](#)]
3. Issemann, I.; Green, S. Activation of a member of the steroid hormone receptor superfamily by peroxisome proliferators. *Nature* **1990**, *347*, 645–650. [[CrossRef](#)] [[PubMed](#)]
4. Sher, T.; Yi, H.F.; McBride, O.W.; Gonzalez, F.J. cDNA cloning, chromosomal mapping, and functional characterization of the human peroxisome proliferator activated receptor. *Biochemistry* **1993**, *32*, 5598–5604. [[CrossRef](#)] [[PubMed](#)]
5. Peters, J.M.; Cheung, C.; Gonzalez, F.J. Peroxisome proliferator-activated receptor- α and liver cancer: Where do we stand? *J. Mol. Med.* **2005**, *83*, 774–785. [[CrossRef](#)] [[PubMed](#)]
6. Poulsen, L.L.; Siersbk, M.; Mandrup, S. PPARs: Fatty acid sensors controlling metabolism. *Semin. Cell Dev. Biol.* **2012**, *23*, 631–639. [[CrossRef](#)]
7. Biddie, S.C.; John, S.; Hager, G.L. Genome-wide mechanisms of nuclear receptor action. *Trends Endocrinol. Metab.* **2010**, *21*, 3–9. [[CrossRef](#)]
8. Hager, G.L.; Varticovski, L. Chromatin in time and space. *Biochim. Biophys. Acta* **2012**, *1819*, 631. [[CrossRef](#)]
9. Peters, J.M.; Shah, Y.M.; Gonzalez, F.J. The role of peroxisome proliferator-activated receptors in carcinogenesis and chemoprevention. *Nat. Rev. Cancer* **2012**, *12*, 181–195. [[CrossRef](#)]
10. Qiu, Y.Y.; Zhang, J.; Zeng, F.Y.; Zhu, Y.Z. Roles of the peroxisome proliferator-activated receptors (PPARs) in the pathogenesis of nonalcoholic fatty liver disease (NAFLD). *Pharmacol. Res.* **2023**, *192*, 106786. [[CrossRef](#)]
11. Souza-Tavares, H.; Miranda, C.S.; Vasques-Monteiro, I.M.L.; Sandoval, C.; Santana-Oliveira, D.A.; Silva-Veiga, F.M.; Fernandes-da-Silva, A.; Souza-Mello, V. Peroxisome proliferator-activated receptors as targets to treat metabolic diseases: Focus on the adipose tissue, liver, and pancreas. *World J. Gastroenterol.* **2023**, *29*, 4136–4155. [[CrossRef](#)]
12. Kersten, S.; Seydoux, J.; Peters, J.M.; Gonzalez, F.J.; Desvergne, B.; Wahli, W. Peroxisome proliferator-activated receptor α mediates the adaptive response to fasting. *J. Clin. Investig.* **1999**, *103*, 1489–1498. [[CrossRef](#)]

13. Foreman, J.E.; Koga, T.; Kosyk, O.; Kang, B.-H.; Zhu, X.; Cohen, S.M.; Billy, L.J.; Sharma, A.; Amin, S.; Gonzalez, F.J.; et al. Differential hepatocarcinogenesis by a potent, high affinity human PPAR α agonist in PPARA-humanized mice. *Toxicol. Sci.* **2021**, *183*, 70–80. [[CrossRef](#)] [[PubMed](#)]
14. Foreman, J.E.; Koga, T.; Kosyk, O.; Kang, B.-H.; Zhu, X.; Cohen, S.M.; Billy, L.J.; Sharma, A.; Amin, S.; Gonzalez, F.J.; et al. Species differences between mouse and human PPAR α in modulating the hepatocarcinogenic effects of perinatal exposure to a high affinity human PPAR α agonist in mice. *Toxicol. Sci.* **2021**, *183*, 81–92. [[CrossRef](#)]
15. Hays, T.; Rusyn, I.; Burns, A.M.; Kennett, M.J.; Ward, J.M.; Gonzalez, F.J.; Peters, J.M. Role of peroxisome proliferator-activated receptor- α (PPAR α) in bezafibrate-induced hepatocarcinogenesis and cholestasis. *Carcinogenesis* **2005**, *26*, 219–227. [[CrossRef](#)]
16. Morimura, K.; Cheung, C.; Ward, J.M.; Reddy, J.K.; Gonzalez, F.J. Differential susceptibility of mice humanized for peroxisome proliferator-activated receptor α to Wy-14,643-induced liver tumorigenesis. *Carcinogenesis* **2006**, *27*, 1074–1080. [[CrossRef](#)] [[PubMed](#)]
17. Peters, J.M.; Cattley, R.C.; Gonzalez, F.J. Role of PPAR α in the mechanism of action of the nongenotoxic carcinogen and peroxisome proliferator Wy-14,643. *Carcinogenesis* **1997**, *18*, 2029–2033. [[CrossRef](#)] [[PubMed](#)]
18. Aibara, D.; Takahashi, S.; Yagai, T.; Kim, D.; Brocker, C.N.; Levi, M.; Matsusue, K.; Gonzalez, F.J. Gene repression through epigenetic modulation by PPARA enhances hepatocellular proliferation. *iScience* **2022**, *25*, 104196. [[CrossRef](#)]
19. Peters, J.M.; Aoyama, T.; Cattley, R.C.; Nobumitsu, U.; Hashimoto, T.; Gonzalez, F.J. Role of peroxisome proliferator-activated receptor α in altered cell cycle regulation in mouse liver. *Carcinogenesis* **1998**, *19*, 1989–1994. [[CrossRef](#)]
20. Shah, Y.M.; Morimura, K.; Yang, Q.; Tanabe, T.; Takagi, M.; Gonzalez, F.J. Peroxisome proliferator-activated receptor α regulates a microRNA-mediated signaling cascade responsible for hepatocellular proliferation. *Mol. Cell Biol.* **2007**, *27*, 4238–4247. [[CrossRef](#)]
21. Corton, J.C.; Peters, J.M.; Klaunig, J.E. The PPAR α -dependent rodent liver tumor response is not relevant to humans: Addressing misconceptions. *Arch. Toxicol.* **2018**, *92*, 83–119. [[CrossRef](#)] [[PubMed](#)]
22. Klaunig, J.E.; Babich, M.A.; Baetcke, K.P.; Cook, J.C.; Corton, J.C.; David, R.M.; DeLuca, J.G.; Lai, D.Y.; McKee, R.H.; Peters, J.M.; et al. PPAR α agonist-induced rodent tumors: Modes of action and human relevance. *Crit. Rev. Toxicol.* **2003**, *33*, 655–780. [[CrossRef](#)] [[PubMed](#)]
23. Tateno, C.; Yamamoto, T.; Utoh, R.; Yamasaki, C.; Ishida, Y.; Myoken, Y.; Oofusa, K.; Okada, M.; Tsutsui, N.; Yoshizato, K. Chimeric mice with hepatocyte-humanized liver as an appropriate model to study human peroxisome proliferator-activated receptor- α . *Toxicol. Pathol.* **2015**, *43*, 233–248. [[CrossRef](#)]
24. Howroyd, P.; Swanson, C.; Dunn, C.; Cattley, R.C.; Corton, J.C. Decreased longevity and enhancement of age-dependent lesions in mice lacking the nuclear receptor peroxisome proliferator-activated receptor α (PPAR α). *Toxicol. Pathol.* **2004**, *32*, 591–599. [[CrossRef](#)]
25. Aoyama, T.; Peters, J.; Iritani, N.; Nakajima, T.; Furihata, K.; Hashimoto, T.; Gonzalez, F. Altered constitutive expression of fatty acid-metabolizing enzymes in mice lacking the peroxisome proliferator-activated receptor α (PPAR α). *J. Biol. Chem.* **1998**, *273*, 5678–5684. [[CrossRef](#)]
26. Baffy, G.; Brunt, E.M.; Caldwell, S.H. Hepatocellular carcinoma in non-alcoholic fatty liver disease: An emerging menace. *J. Hepatol.* **2012**, *56*, 1384–1391. [[CrossRef](#)]
27. Ganguly, S.; Muench, G.A.; Shang, L.; Rosenthal, S.B.; Rahman, G.; Wang, R.; Wang, Y.; Kwon, H.C.; Diomino, A.M.; Kisseleva, T.; et al. Nonalcoholic Steatohepatitis and HCC in a Hyperphagic Mouse Accelerated by Western Diet. *Cell Mol. Gastroenterol. Hepatol.* **2021**, *12*, 891–920. [[CrossRef](#)]
28. Zhong, F.; Zhou, X.; Xu, J.; Gao, L. Rodent Models of Nonalcoholic Fatty Liver Disease. *Digestion* **2020**, *101*, 522–535. [[CrossRef](#)] [[PubMed](#)]
29. Brown, P.J.; Smith-Oliver, T.A.; Charifson, P.S.; Tomkinson, N.C.; Fivush, A.M.; Sternbach, D.D.; Wade, L.E.; Orband-Miller, L.; Parks, D.J.; Blanchard, S.G.; et al. Identification of peroxisome proliferator-activated receptor ligands from a biased chemical library. *Chem. Biol.* **1997**, *4*, 909–918. [[CrossRef](#)]
30. Akiyama, T.E.; Nicol, C.J.; Fievet, C.; Staels, B.; Ward, J.M.; Auwerx, J.; Lee, S.S.; Gonzalez, F.J.; Peters, J.M. Peroxisome proliferator-activated receptor- α regulates lipid homeostasis, but is not associated with obesity: Studies with congenic mouse lines. *J. Biol. Chem.* **2001**, *276*, 39088–39093. [[CrossRef](#)]
31. Cheung, C.; Akiyama, T.E.; Ward, J.M.; Nicol, C.J.; Feigenbaum, L.; Vinson, C.; Gonzalez, F.J. Diminished hepatocellular proliferation in mice humanized for the nuclear receptor peroxisome proliferator-activated receptor- α . *Cancer Res.* **2004**, *64*, 3849–3854. [[CrossRef](#)] [[PubMed](#)]
32. Tremblay, J.; Hamet, P. Impact of genetic and epigenetic factors from early life to later disease. *Metabolism* **2008**, *57* (Suppl. S2), S27–S31. [[CrossRef](#)]
33. Cibelli, A.; Stefanini, S.; Ceru, M.P. Peroxisomal beta-oxidation and catalase activities in fetal rat liver: Effect of maternal treatment with clofibrate. *Cell Mol. Biol.* **1988**, *34*, 191–205. [[PubMed](#)]
34. Dostal, L.A.; Jenkins, W.L.; Schwetz, B.A. Hepatic peroxisome proliferation and hypolipidemic effects of di(2-ethylhexyl)phthalate in neonatal and adult rats. *Toxicol. Appl. Pharmacol.* **1987**, *87*, 81–90. [[CrossRef](#)] [[PubMed](#)]
35. Stefanini, S.; Mauriello, A.; Farrace, M.G.; Cibelli, A.; Ceru, M.P. Proliferative response of foetal liver peroxisomes to clofibrate treatment of pregnant rats. A quantitative evaluation. *Biol. Cell* **1989**, *67*, 299–305. [[CrossRef](#)]
36. Stefanini, S.; Nardacci, R.; Farioli-Vecchioli, S.; Pajalunga, D.; Sartori, C. Liver and kidney peroxisomes in lactating rats and their pups after treatment with ciprofibrate. Biochemical and morphometric analysis. *Cell Mol. Biol.* **1999**, *45*, 815–829.

37. Alexandri, E.; Ahmed, R.; Siddiqui, H.; Choudhary, M.I.; Tsiafoulis, C.G.; Gerothanassis, I.P. High Resolution NMR Spectroscopy as a Structural and Analytical Tool for Unsaturated Lipids in Solution. *Molecules* **2017**, *22*, 1663. [[CrossRef](#)]
38. Casu, M.; Anderson, G.J.; Gibbons, W.A. NMR lipid profiles of cells, tissues and body fluids. I— 1D and 2D Proton NMR of lipids from rat liver. *Magn. Reson. Chem.* **1991**, *29*, 594–602. [[CrossRef](#)]
39. Feng, J.; Isern, N.G.; Burton, S.D.; Hu, J.Z. Studies of Secondary Melanoma on C57BL/6J Mouse Liver Using 1H NMR Metabolomics. *Metabolites* **2013**, *3*, 1011–1035. [[CrossRef](#)]
40. Jiang, C.Y.; Yang, K.M.; Yang, L.; Miao, Z.X.; Wang, Y.H.; Zhu, H.B. A (1)H NMR-Based Metabonomic Investigation of Time-Related Metabolic Trajectories of the Plasma, Urine and Liver Extracts of Hyperlipidemic Hamsters. *PLoS ONE* **2013**, *8*, e66786. [[CrossRef](#)]
41. Xu, Z.; Harvey, K.; Pavlina, T.; Dutot, G.; Zaloga, G.; Siddiqui, R. An improved method for determining medium- and long-chain FAMES using gas chromatography. *Lipids* **2010**, *45*, 199–208. [[CrossRef](#)] [[PubMed](#)]
42. Zhang, L.; Rimal, B.; Nichols, R.G.; Tian, Y.; Smith, P.B.; Hatzakis, E.; Chang, S.C.; Butenhoff, J.L.; Peters, J.M.; Patterson, A.D. Perfluorooctane sulfonate alters gut microbiota-host metabolic homeostasis in mice. *Toxicology* **2020**, *431*, 152365. [[CrossRef](#)] [[PubMed](#)]
43. Borland, M.G.; Foreman, J.E.; Girroir, E.E.; Zolfaghari, R.; Sharma, A.K.; Amin, S.M.; Gonzalez, F.J.; Ross, A.C.; Peters, J.M. Ligand Activation of Peroxisome Proliferator-Activated Receptor- β/δ (PPAR β/δ) Inhibits Cell Proliferation in Human HaCaT Keratinocytes. *Mol. Pharmacol.* **2008**, *74*, 1429–1442. [[CrossRef](#)] [[PubMed](#)]
44. Aguilar Diaz De Leon, J.; Borges, C.R. Evaluation of Oxidative Stress in Biological Samples Using the Thiobarbituric Acid Reactive Substances Assay. *J. Vis. Exp.* **2020**, *159*, e61122. [[CrossRef](#)]
45. Brown, Z.J.; Fu, Q.; Ma, C.; Kruhlak, M.; Zhang, H.; Luo, J.; Heinrich, B.; Yu, S.J.; Zhang, Q.; Wilson, A.; et al. Carnitine palmitoyltransferase gene upregulation by linoleic acid induces CD4(+) T cell apoptosis promoting HCC development. *Cell Death Dis.* **2018**, *9*, 620. [[CrossRef](#)]
46. Jin, R.; Hao, J.; Yi, Y.; Yin, D.; Hua, Y.; Li, X.; Bao, H.; Han, X.; Egilmez, N.K.; Sauter, E.R.; et al. Dietary Fats High in Linoleic Acids Impair Antitumor T-cell Responses by Inducing E-FABP-Mediated Mitochondrial Dysfunction. *Cancer Res.* **2021**, *81*, 5296–5310. [[CrossRef](#)]
47. Ma, C.; Kesarwala, A.H.; Eggert, T.; Medina-Echeverez, J.; Kleiner, D.E.; Jin, P.; Stroncek, D.F.; Terabe, M.; Kapoor, V.; ElGindi, M.; et al. NAFLD causes selective CD4(+) T lymphocyte loss and promotes hepatocarcinogenesis. *Nature* **2016**, *531*, 253–257. [[CrossRef](#)]
48. Reddy, J.K.; Azarnoff, D.L.; Hignite, C.E. Hypolipidaemic hepatic peroxisome proliferators form a novel class of chemical carcinogens. *Nature* **1980**, *283*, 397–398. [[CrossRef](#)]
49. Corton, J.C.; Cunningham, M.L.; Hummer, B.T.; Lau, C.; Meek, B.; Peters, J.M.; Popp, J.A.; Rhomberg, L.; Seed, J.; Klaunig, J.E. Mode of action framework analysis for receptor-mediated toxicity: The peroxisome proliferator-activated receptor α (PPAR α) as a case study. *Crit. Rev. Toxicol.* **2014**, *44*, 1–49. [[CrossRef](#)]
50. Sun, J.; Yu, L.; Qu, X.; Huang, T. The role of peroxisome proliferator-activated receptors in the tumor microenvironment, tumor cell metabolism, and anticancer therapy. *Front. Pharmacol.* **2023**, *14*, 1184794. [[CrossRef](#)]
51. Meek, M.E.; Berry, C.; Boobis, A.R.; Cohen, S.M.; Hartley, M.; Munn, S.; Olin, S.; Schlatter, J.; Vickers, C. Re: Guyton, Kathryn Z., Barone, Stanley, Jr., Brown, Rebecca C., Euling, Susan Y., Jinot, Jennifer, Makris, Susan (2008). Mode of action frameworks: A critical analysis. *Journal of Toxicology and Environmental Health, Part B*, 11(1): 16-31. *J. Toxicol. Environ. Health B Crit. Rev.* **2008**, *11*, 681–683. [[CrossRef](#)] [[PubMed](#)]
52. Kersten, S. Integrated physiology and systems biology of PPAR α . *Mol. Metab.* **2014**, *3*, 354–371. [[CrossRef](#)]
53. Kersten, S.; Stienstra, R. The role and regulation of the peroxisome proliferator activated receptor alpha in human liver. *Biochimie* **2017**, *136*, 75–84. [[CrossRef](#)]
54. Peters, J.M.; Hennuyer, N.; Staels, B.; Fruchart, J.C.; Fievet, C.; Gonzalez, F.J.; Auwerx, J. Alterations in lipoprotein metabolism in peroxisome proliferator-activated receptor α -deficient mice. *J. Biol. Chem.* **1997**, *272*, 27307–27312. [[CrossRef](#)]
55. Fu, Y.; Chung, F.L. Oxidative stress and hepatocarcinogenesis. *Hepatoma Res.* **2018**, *4*, 39. [[CrossRef](#)]
56. Kang, T.W.; Yevsa, T.; Woller, N.; Hoenicke, L.; Wuestefeld, T.; Dauch, D.; Hohmeyer, A.; Gereke, M.; Rudalska, R.; Potapova, A.; et al. Senescence surveillance of pre-malignant hepatocytes limits liver cancer development. *Nature* **2011**, *479*, 547–551. [[CrossRef](#)]
57. Braumuller, H.; Wieder, T.; Brenner, E.; Assmann, S.; Hahn, M.; Alkhaled, M.; Schilbach, K.; Essmann, F.; Kneilling, M.; Griessinger, C.; et al. T-helper-1-cell cytokines drive cancer into senescence. *Nature* **2013**, *494*, 361–365. [[CrossRef](#)]
58. Quezada, S.A.; Simpson, T.R.; Peggs, K.S.; Merghoub, T.; Vider, J.; Fan, X.; Blasberg, R.; Yagita, H.; Muranski, P.; Antony, P.A.; et al. Tumor-reactive CD4(+) T cells develop cytotoxic activity and eradicate large established melanoma after transfer into lymphopenic hosts. *J. Exp. Med.* **2010**, *207*, 637–650. [[CrossRef](#)] [[PubMed](#)]
59. Rakhra, K.; Bachireddy, P.; Zabuawala, T.; Zeiser, R.; Xu, L.; Kopelman, A.; Fan, A.C.; Yang, Q.; Braunstein, L.; Crosby, E.; et al. CD4(+) T cells contribute to the remodeling of the microenvironment required for sustained tumor regression upon oncogene inactivation. *Cancer Cell* **2010**, *18*, 485–498. [[CrossRef](#)] [[PubMed](#)]
60. Calzascia, T.; Pellegrini, M.; Hall, H.; Sabbagh, L.; Ono, N.; Elford, A.R.; Mak, T.W.; Ohashi, P.S. TNF-alpha is critical for antitumor but not antiviral T cell immunity in mice. *J. Clin. Investig.* **2007**, *117*, 3833–3845. [[CrossRef](#)]
61. Radaeva, S.; Jaruga, B.; Hong, F.; Kim, W.H.; Fan, S.; Cai, H.; Strom, S.; Liu, Y.; El-Assal, O.; Gao, B. Interferon-alpha activates multiple STAT signals and down-regulates c-Met in primary human hepatocytes. *Gastroenterology* **2002**, *122*, 1020–1034. [[CrossRef](#)]

62. Wakil, A.E.; Wang, Z.E.; Ryan, J.C.; Fowell, D.J.; Locksley, R.M. Interferon gamma derived from CD4(+) T cells is sufficient to mediate T helper cell type 1 development. *J. Exp. Med.* **1998**, *188*, 1651–1656. [[CrossRef](#)]
63. Kale, A.; Sharma, A.; Stolzing, A.; Desprez, P.Y.; Campisi, J. Role of immune cells in the removal of deleterious senescent cells. *Immun. Ageing* **2020**, *17*, 16. [[CrossRef](#)]
64. Mossanen, J.C.; Kohlhepp, M.; Wehr, A.; Krenkel, O.; Liepelt, A.; Roeth, A.A.; Mockel, D.; Heymann, F.; Lammers, T.; Gassler, N.; et al. CXCR6 Inhibits Hepatocarcinogenesis by Promoting Natural Killer T- and CD4(+) T-Cell-Dependent Control of Senescence. *Gastroenterology* **2019**, *156*, 1877–1889.e1874. [[CrossRef](#)]
65. Song, P.; An, J.; Zou, M.H. Immune Clearance of Senescent Cells to Combat Ageing and Chronic Diseases. *Cells* **2020**, *9*, 671. [[CrossRef](#)] [[PubMed](#)]
66. Okuma, A.; Hanyu, A.; Watanabe, S.; Hara, E. p16(Ink4a) and p21(Cip1/Waf1) promote tumour growth by enhancing myeloid-derived suppressor cells chemotaxis. *Nat. Commun.* **2017**, *8*, 2050. [[CrossRef](#)] [[PubMed](#)]
67. Pereira, B.I.; Devine, O.P.; Vukmanovic-Stejic, M.; Chambers, E.S.; Subramanian, P.; Patel, N.; Virasami, A.; Sebire, N.J.; Kinsler, V.; Valdovinos, A.; et al. Senescent cells evade immune clearance via HLA-E-mediated NK and CD8(+) T cell inhibition. *Nat. Commun.* **2019**, *10*, 2387. [[CrossRef](#)] [[PubMed](#)]
68. Liu, Z.; Suo, C.; Jiang, Y.; Zhao, R.; Zhang, T.; Jin, L.; Chen, X. Phenome-Wide Association Analysis Reveals Novel Links Between Genetically Determined Levels of Liver Enzymes and Disease Phenotypes. *Phenomics* **2022**, *2*, 295–311. [[CrossRef](#)]

Disclaimer/Publisher’s Note: The statements, opinions and data contained in all publications are solely those of the individual author(s) and contributor(s) and not of MDPI and/or the editor(s). MDPI and/or the editor(s) disclaim responsibility for any injury to people or property resulting from any ideas, methods, instructions or products referred to in the content.